Electrochemical Activity of Pt Supported on Carbon Black

H. Hatori[a], L. R. Radovic[b], R. R. Adzic[c]

[a]National Institute of Advanced Industrial Science and Technology, 16-1 Onogawa Tsukuba 305-8569, Japan.

[b]Department of Energy and Geo-Environmental Engineering, The Pennsylvania State University, University Park, PA 16802, USA.

[c]Brookhaven National Laboratory, Upton, NY 11973, USA

Introduction

Highly dispersed platinum on carbon black is the best electrocatalyst for O_2 reduction in solid polymer electrolyte fuel cells. Specific mass activity of this catalyst is of considerable importance because of a need to lower the costs of fuel cells by minimizing the Pt loading. Carbon black supported Pt electrocatalysts with Pt particles of varying size were prepared and the electrochemical activity was studied by measuring hydrogen adsorption/desorption and oxygen reduction kinetics in sulfuric acid solutions by means of a rotating disk-ring electrode technique.

Experimental

Preparation and characterization of the catalyst

Carbon black (Vulcan XC-72R) as received or additionally oxidized by nitric acid was used. The total acidic groups on these carbon black samples, measured by Boehm method, were 0.24 and 0.86 mequiv/g, respectively. The Pt nanoparticles were formed by impregnating carbon with H_2PtCl_6 or $[Pt(NH_3)_4](NO_3)_2$, or ion exchange of $[Pt(NH_3)_4](OH)_2$. The samples containing approximately 10wt% and 5wt% of Pt, Pt/C10 and Pt/C5, were prepared; Pt/C10-1 (9.8 wt%): H_2PtCl_6 impregnation on XC-72R as received and drying on hot plate; Pt/C10-2 (10.4 wt%): H_2PtCl_6 impregnation on XC-72R as received and drying at room temperature; Pt/C10-3 (9.6 wt%): H_2PtCl_6 impregnation on the oxidized XC-72R and drying on hot plate; Pt/C10-4 (8.9 wt%): $[Pt(NH_3)_4](NO_3)_2$ impregnation on XC-72R as received and drying on hot plate; Pt/C5-1 (5.0 wt%): ion exchange of $[Pt(NH_3)_4](OH)_2$ on the oxidized XC-72R and drying after filtration. The dried samples were reduced in H_2 at 200°C for 2 h. The content of Pt in parenthesis was measured by X-ray fluorescence analysis. Commercial available catalyst (ETEK10), 9.7wt% Pt on Vulcan XC-72R, was also used.

The particle size and the surface area (SA) of platinum on carbon black were estimated by X-ray diffraction (XRD) and transmission electron microscopy (TEM). The SA_{XRD} and SA_{TEM} are shown in Table 1 with the crystallite size L_{111} given from the XRD profiles and the average diameter d_{ave} determined by TEM observations.

A RRDE preparation and electrochemical measurements

The thin catalyst layer was prepared on RRDE by the method reported [1, 2]. A RRDE with glassy carbon disk (5mm diameter, 0.196 cm^2) and gold ring was used after polishing before each experiment. Suspensions of 2mg-catalyst/ml were produced by ultrasonically dispersing of a 50 mg catalyst in pure water or 10%-methanol/H_2O, depending on the stability of the suspension. A 0.01ml of the suspension was pipetted onto glassy carbon disk and dried. In case of Pt/C5-1D, the deposition of catalyst is repeated twice and hence the loading amount of the catalyst is doubled on the disk. A 0.01ml of a diluted Nafion solution (1/50 dilution of the 5wt% commercial available solution, Aldrich) was put on the dried catalyst layer. After evaporation of the solvent, the electrode was used for the electrochemical measurements.

Potentials were measured using the reversible hydrogen electrode (RHE). The electrolyte used was 0.5M H_2SO_4. Steady-state cyclic voltammograms (CV) were measured under nitrogen atmosphere at a sweep rate of 50 mV/s. The charge (Q_{H+}) and the active surface area (SA_{CV}) in Table 1 is given from the hydrogen adsorption/desorption peaks. The SA_{CV} was calculated assuming that charge of 0.22 mC/cm^2 corresponds to a monolayer of adsorbed hydrogen atoms. After the measurement of the steady-state cyclic voltammograms, the polarization curves were recorded using the same electrode by linear-sweep technique with the rate of 10 mV/s and a rotation range of 225-2500 rpm. The potential of the ring was kept at 1.2 mV during the linear-sweep of the disk electrode from the potential of 1.1-0.05V. Since the current recorded in O_2 atmosphere includes a background current due to double-layer charging, Pt oxide formation/reduction and H_2SO_4 adsorption/desorption, the polarization curves for O_2 reduction were corrected by subtraction of the background currents measured in N_2 atmosphere.

Results and Discussion

Particle size and Dispersion of Pt on carbon

The dispersion of Pt in Pt/C10-1 was excellent as is shown in TEM micrograph (Fig. 1a). The average particle diameter d_{ave} given from the particle size distribution corresponded well to the average crystallite size L_{111} measured by XRD. The ion exchange condition also yielded a sample Pt/C5-1 with excellent dispersion of Pt particles. On the other hand, the Pt size and the distribution became large and broad in the order of Pt/C10-1<Pt/C10-2<Pt/C10-3<Pt/C10-4. The disagreement between L_{111} and d_{ave} is due to the broad distribution of Pt particle size, that is, the XRD profile dominantly reflects the diffraction from the larger particles. The aggregate of Pt in Pt/C10-4 was occasionally more than 20nm and the dispersion was too inhomogeneous to measure the size distribution by TEM. When $[Pt(NH_3)_4](NO_3)_2$ was used, the Pt cation in no ion exchange condition has lower interaction with carbon surface and hence the salt would be gathered to each other during the drying process in the impregnation.

In case of the impregnation of H_2PtCl_6, the Pt particle size and the distribution were largely changed by the oxidation of the carrier XC-72R. In Pt/C10-3, the Pt particles with 6-8nm in size were aggregated on a specific part as is shown in Fig. 1b. That is to say, oxidation of carbon surface caused an inhomogeneity of Pt dispersion. The aggregation occurs on a disordered carbon microtexture (Fig. 1c), while the particles were dispersed on the typical microtexture of carbon black (Fig. 1d). The phenomena is explained as follows; the interaction between Pt anion and H_2O is stronger than that between Pt anion and carbon surface, or that between H_2PtCl_6. This means the behavior of H_2O on carbon black during the drying process is important. The specific part on carbon with less crystallinity, which is generated by HNO_3 oxidation, is considered to have higher hydrophilicity because of oxygen functional groups, and hence the H_2PtCl_6 hydrated is gathered at the part.

Electrochemical activity of Pt/C

The polarization curve of the ring electrode and the disk electrode with Pt/C10-1 catalyst layer is shown in Fig. 2. The current observed at lower potentials on the curve of ring electrode is due to the oxidation reaction of H_2O_2 formed by the O_2 reduction on disk by the two-electron mechanism. The ring current tended to increase with the increase of rotation rate, but the current was too small even at 2500 rpm compared to that of ORR on disk electrode. The ORR reaction on the thin catalyst layer on the disk electrode is basically considered to proceed by four-electron mechanism. The polarization curves showed a significant hysteresis; the ORR activity in cathodic sweep is lower than in anodic sweep. The same hysteresis has been reported for Pt supported on carbon, and was explained by the slower oxidation reaction on the oxidized Pt surface than the reduced surface [3].

Levich-Koutechy plots given from the polarization curves (anodic sweep) on disk electrode with Pt/C10-1 catalyst layer is shown in Fig. 3. The intercept of the plot for limiting current is near to zero, indicating the low diffusion current controlled by the film thickness of Nafion coated [2]. The parallel lines of these plots show that the number of electron transferred does not change at the potential range. The kinetic current I_{kin} is also given from the intercept of the plot for the potential at 0.9 V. The I_{kin}, mass activity ($A_{mass} = I_{kin}$/g-Pt) and specific activity ($A_{specific} = A_{mass} / SA_{CV}$) at 0.9 V is listed in Table 1. The lower I_{kin} of the Pt/C5-1 than Pt/C10-1 was clearly shown when the same amount of catalyst was loaded on the disk. On the other hand, the I_{kin} of Pt/C5-1D and Pt/C10-1 which had the same amount of Pt loaded on disk electrode were comparable to each other. The oxygen reduction kinetics was found largely independent of the active surface area; the mass activity was approximately constant for the samples with different size of Pt particles and different active surface area SA_{CV} given from the electrochemical hydrogen adsorption/desorption. For example, the difference of mass activity between Pt/C10-1 and Pt/C10-3 was basically negligible though Pt/C10-3 had the AS_{CV} less than the half of Pt/C10-1. As a result, the tendency, the decrease of specific activity with decreasing particle size, was appeared. The independence of mass activity on Pt particle size is in agreement with data in ref. [2-4] and is probably explained by the structure-sensitive-adsorption of sulfate/bisulfate anions.

Acknowledgement

One of the author (H. Hatori) is grateful to Agency of Science and Technology, Japan. The present work was partly supported by the Japan Society for the Promotion of Science under RFTF program No. JSPS-RFTF96R11701.

References

1. Schmidt TJ, Gasteiger HA, Stab GD, Urban PM, Kolb DM, Behm RJ. J Electrochem Soc 1998; 145(7): 2354-2358.
2. Paulus UA, Schmidt TJ, Gasteiger HA, Behm RJ. J Electroanalytical Chem 2001; 495: 134-145.
3. Gojkovic SL, Zecevic SK, Savinell RF. J Electrochem Soc 1998; 145(11): 3713-3720.
4. Markovic N, Gasteiger H, Ross PN. J Electrochem Soc 1997; 144:1591

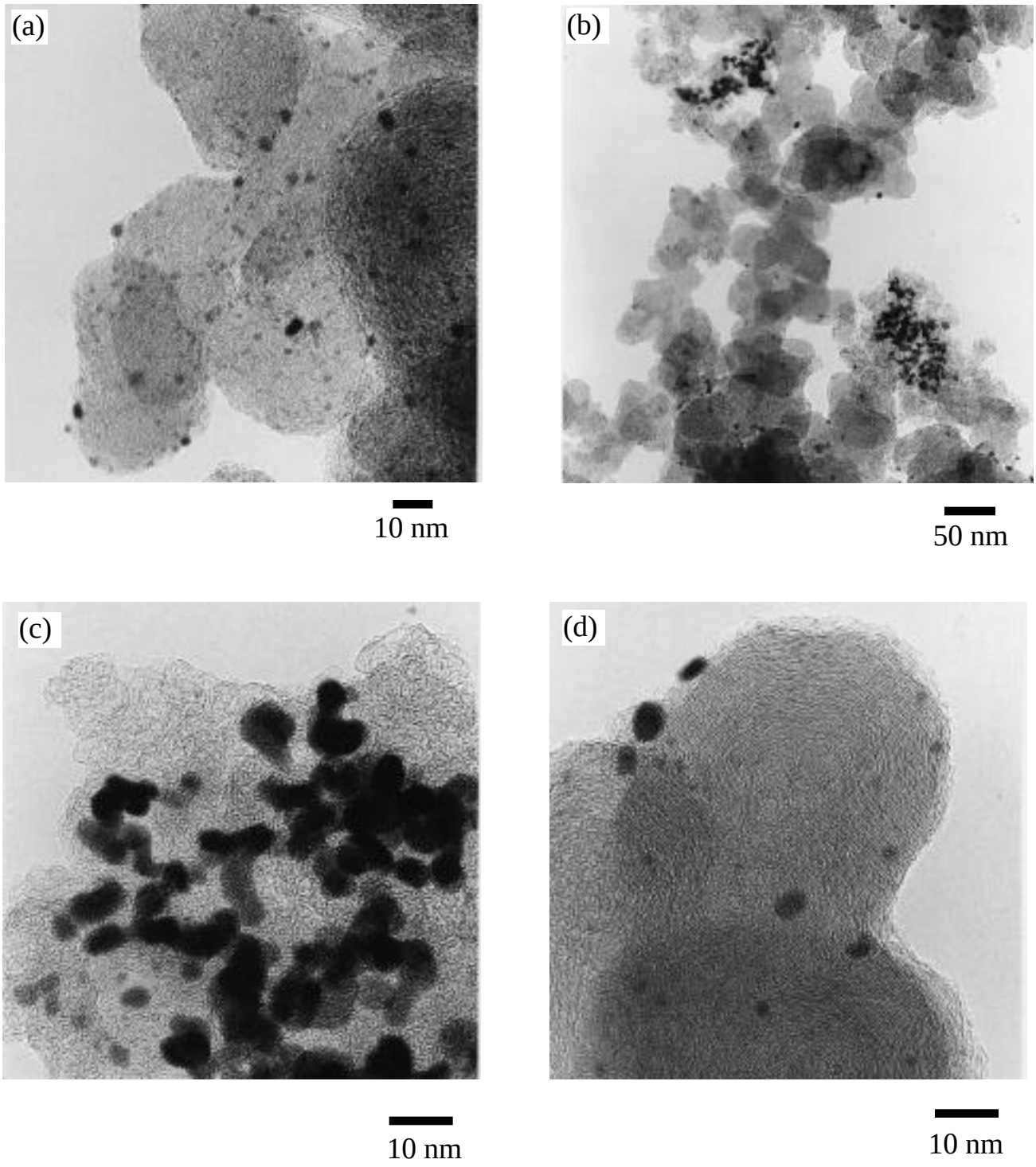

Fig. 1. TEM micrographs of (a) Pt/C10-1 and (b)-(d) Pt/C10-3. The large Pt particles in Pt/C10-3 gathered on the disordered carbon texture (c) and were a few on the typical microtexture of carbon black (d).

Table 1. Surface areas and ORR activity. The surface areas were measured by XRD, TEM and proton adsorption. The SA_{H+} was used for the calculation of the $A_{specific}$.

	XRD		TEM[*1]		CV[*2]		ORR activity at 0.9V[*3]		
	L_{111} (nm)	SA_{XRD} (m^2/g-Pt)	d_{ave} (nm)	SA_{TEM} (m^2/g-Pt)	Q_{H+} (mC)	SA_{CV} (m^2/g-Pt)	I_{kin} (μA)	A_{mass} (A/g-Pt)	$A_{specific}$ (A/m^2-Pt)
Pt/C10-1	1.7	165	1.6	178	0.66	144	106	51	0.35
Pt/C10-2	4.0	70	2.3	125	0.46	94	97	47	0.47
Pt/C10-3	7.4	38	2.9	96	0.30	67	96	47	0.70
Pt/C10-4	10.2	27	-[*4]	-[*4]	0.28	67	17	7	0.10
ETEK10	2 and 7[*5]	-	1.9	150	0.38	83	81	38	0.45
Pt/C5-1	<1.5	>187	1.3	209	0.29	124	41	39	0.31
Pt/C5-1D					0.66	142	93	44	0.31

*1: The d_{ave} and SA_{TEM} calculated from the particle size distribution given by TEM observations.
*2: Proton adsorption/desorption in 0.5M H_2SO_4. Sweep rate 50mV/s.
*3: ORR in O_2-saturated 0.5M H_2SO_4 at 25˚C. Sweep rate 10mV/s.
*4: A composite profile was given; one is from the particles of about 2nm and the other is from those of about 7nm.
*5: Aggregation of Pt and the size distribution were too large and broad to measure d_{ave} and SA_{TEM}.

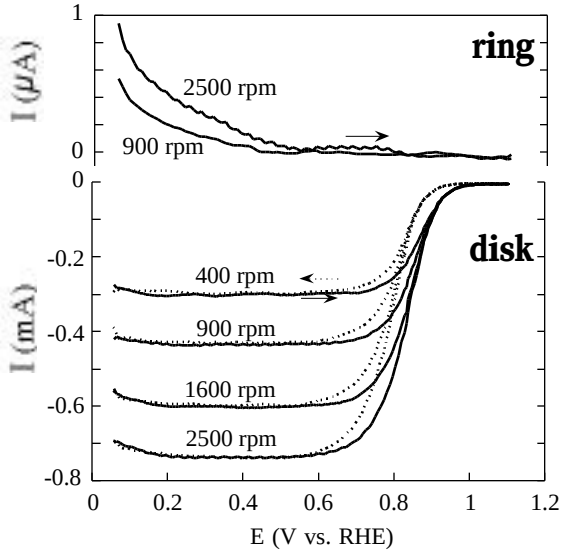

Fig. 2. Polarization curves for O_2 reduction on Pt/C10-1 at different rotation rates in cathodic and anodic sweep directions. Sweep rate 10 mV/s.

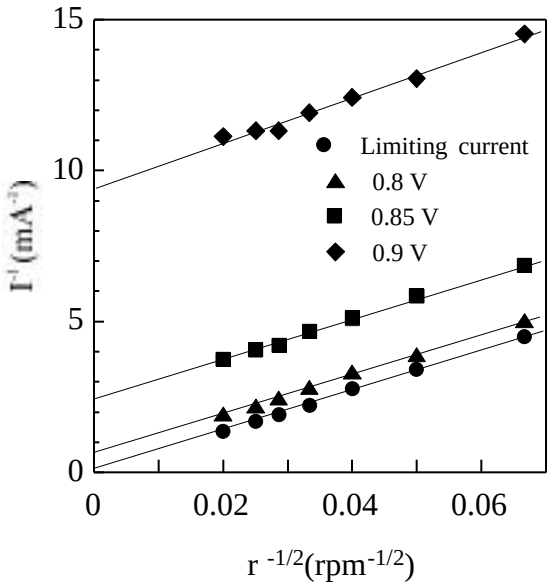

Fig. 3. Levic-Koutecky plots for O_2 reduction on Pt/C10-1, given from the data in Fig. 2 (anodic sweep direction).